Mitochondrial content is preserved throughout disease progression in the mdx mouse model of Duchenne muscular dystrophy, regardless of taurine supplementation

Barker, RG, Wyckelsma, Victoria, Xu, H and Murphy, RM (2018) Mitochondrial content is preserved throughout disease progression in the mdx mouse model of Duchenne muscular dystrophy, regardless of taurine supplementation. American Journal of Physiology - Cell Physiology, 314 (4). 483 - 491. ISSN 0363-6143

Mitochondrial content is preserved throughout disease progression in the *mdx* mouse model of Duchenne muscular dystrophy, regardless of taurine supplementation

Robert G. Barker[1], Victoria L. Wyckelsma[1], Hongyang Xu[1] and Robyn M. Murphy[1]

[1]Department of Biochemistry and Genetics, La Trobe Institute for Molecular Science La Trobe University, Melbourne, VIC 3086, Australia.

Correspondence:
Assoc Prof Robyn M. Murphy,
Department of Biochemistry and Genetics,
La Trobe Institute for Molecular Science,
La Trobe University, Melbourne,
Victoria, 3086 Australia,
Telephone: +61-3-9479-2302;
Email: r.murphy@latrobe.edu.au

Running title: Mitochondria in *mdx* mice

Keywords: DMD; *mdx* mouse; Taurine; Skeletal Muscle; Animal Model; mitochondria

Abstract

Mitochondrial dysfunction is a pathological feature of Duchenne muscular dystrophy (DMD), a debilitating and fatal neuromuscular disorder characterised by progressive muscle wasting and weakness. Mitochondria are a source of cellular ATP, involved in Ca^{2+} regulation and apoptotic signalling. Ameliorating aberrant mitochondrial function has therapeutic potential for reducing DMD disease severity. The dystrophic *mdx* mouse exhibits peak muscle damage at 21-28d which stabilises after 8 weeks. The amino acid taurine is implicated in mitochondrial health and function, with endogenous concentrations low when measured during the cycle of peak muscle damage in *mdx* mice. Using whole soleus and EDL muscle homogenates from 28- and 70-d *mdx* mice there was no change in native state mitochondrial complexes using Blue Native-PAGE. NADH:ubiquinone oxidotreductase subunit-A9 (NDUFA9) protein abundance was lower in soleus muscle of 28 and 70 d *mdx* mice and EDL muscle of 70 d *mdx* mice compared to same muscles in WT (C57BL10/ScSn) animals. There were age dependant increases in both NDUFA9 protein abundance and citrate synthase activity in soleus muscles of *mdx* and WT mice. There was no change in abundances of mitochondrial dynamics proteins mitofusin 2 (Mfn2) and mitochondrial dynamics protein 49 (MiD49). Taurine administration essentially did not affect any measurements of mitochondria. Collectively these findings suggest mitochondrial content and dynamics are not reduced in the *mdx* mouse regardless of disease severity. We also elucidate that taurine affords no significant benefit to mitochondrial content or dynamics in the *mdx* mouse at either 28 or 70 d.

Abbreviations : Blue native polyacrylamide gel electrophoresis (BN-PAGE); bovine serum albumin (BSA); citrate synthase (CS); cytochrome C oxidase subunit IV (COX IV); Days (d); Development Studies Hybridoma Bank (DSHB); Duchenne muscular dystrophy (DMD); extensor digitorum longus (EDL); mitochondrial ATP production rate (MAPR); mitochondrial dynamics protein 49 (MiD49); mitofusin 2 (Mfn2); NADH:ubiquinone oxidotreductase subunit-A9 (NDUFA9); oxidative phosphorylation (OXPHOS); phosphate buffered saline (PBS); phosphate buffered saline with 0.025% Tween (PBST); reactive oxygen species (ROS); sarcoplasmic reticulum (SR); SR-calcium ATPase (SERCA); standard deviation (SD); taurine (tau); Tris-buffered, saline-Tween (TBST); Wild type (WT, C57/BL10ScSn)

Introduction

Duchenne Muscular Dystrophy (DMD) is a debilitating, progressive and ultimately fatal neuromuscular disorder affecting approximately 1:3600 live male births (5). Caused by the absence of the protein dystrophin and the subsequent weakening of the sarcolemma, an influx of extracellular Ca^{2+} precedes myofibre necrosis and subsequently progressive muscle wasting and weakness with age (1). The dystrophin deficient *mdx* mouse is a well-established animal model of DMD and exhibits many of the pathophysiological symptoms associated with the disorder (12). It doesn't, however, experience progressive muscle wasting and weakness but rather exhibits an age dependant disease severity, peaking at 21-28 (d)ays at which time it most closely mimics the severity of DMD, before undergoing successful muscle regeneration and stabilising into adulthood (> 8 weeks)(12).

The structural hypothesis for damage in DMD is centred on this Ca^{2+} entry and is widely recognised to precede many of the pathological features seen with DMD (1). Intracellular Ca^{2+} is continuously sequestered into the specialised membrane bound store, the sarcoplasmic reticulum (SR) by the SR-calcium ATPase (SERCA), and hence has a reliance on ATP supply for continued function. A further key aspect of dystrophic muscle is the increased requirement for muscle regeneration as the tissue attempts to repair itself, and this is another significant ATP consuming pathway in the cell.

Mitochondria are the source of cellular energy, producing ATP through a series of five multimeric enzyme complexes termed oxidative phosphorylation (OXPHOS) and play an important role in most cells. The function of each of these complexes is dependent on the efficient assembly of up to 45 different proteins into a single complex (e.g. complex I, (20)). The application of blue native polyacrylamide gel electrophoresis (BN-PAGE) allows these complexes to be visualised. Not only critical to the production of cellular energy via OXPHOS, mitochondria are also regulators of Ca^{2+} homeostasis, a source of reactive oxygen species (ROS) production and act as a regulator of apoptotic signalling (4, 13). Mitochondrial dysfunction has been suspected to be an important pathogenic feature in Duchenne muscular dystrophy (18, 23). Potential mechanisms of this contribution could be a result of the sustained increase in cytosolic Ca^{2+} in dystrophic muscle exerting a Ca^{2+} overload on the

mitochondrial transition pore which eventuates in apoptosis (8) and a consequent decreased ability to produce ATP.

It has been suggested that mitochondria could be a therapeutic target for reducing the severity of symptoms in DMD patients (30). Resting ATP content of dystrophic muscle was reported to be ~50% of that seen in a healthy cohort (2, 6). This could be due to a decreased ability to produce ATP, as analyses of isolated or enriched mitochondrial preparations demonstrated a reduction in mitochondrial ATP production rate (MAPR) and OXPHOS capacity in the *mdx* mouse (18, 30, 32). The decline in ATP could also be due to the increased rate of ATP consumption, for such processes as driving the increased SERCA activity necessary to try and maintain Ca^{2+} homeostasis and/or increased muscle regeneration.

While not completely understood, it has further been suggested that the reduced bioenergetic status presented by the reduced ATP in dystrophic muscle may be attributable to morphologically compromised mitochondria, such as becoming swollen, which alters mitochondrial function (23). Necessary for mitochondrial fusion, mitofusin 2 (Mfn2) is responsible for the maintenance of healthy mitochondrial function, fusing together damaged mitochondria that would otherwise contribute to excess ROS production and subsequent muscle damage (33). Mfn2 was increased in the EDL and diaphragm of the utrophin- dystrophin deficient mouse (29), although it is not known if this is altered in muscle from the less severely affected *mdx* mouse. Whilst studies investigating mitochondrial dynamics previously have examined different proteins involved in mitochondrial fission, such as Fis1 and Opa1, these proteins are also involved in the fission of other organelles, such as peroxisomes and so it is not possible to relate findings specifically to mitochondria (21). Recently, mitochondrial dynamics protein 49 (MiD49) and MiD51 were identified as mitochondrial specific proteins for fission, involved in recruiting Drp1 to the outer mitochondrial membrane (31). MiD49 has only recently been described in skeletal muscle (39) and whether it is altered in dystrophic muscle is not known.

Taurine is an amino acid found ubiquitously in all mammalian cells, and whilst not classified as essential has extensively been characterised as vital for healthy muscle function and development (9, 16). Dystrophin deficiency has been shown to impact taurine metabolism

(34). In the *mdx* mouse limb muscle taurine levels have been found to be reduced both before and during the onset of severe dystropathology (21-28 d), before returning to endogenous levels as the pathology stabilises into adulthood (70 d) (11, 22). The availability of sufficient taurine both before and during these critical stages is therefore an area of interest for the potential attenuation of the dystrophic pathology shown in the *mdx* mouse. Taurine deficiency has been studied using a taurine transporter knockout mouse where intramuscular taurine is almost absent (37). Such studies demonstrate pathological symptoms indicative of those seen with dystrophin deficiency, indicating that taurine has a role in mitochondrial function and energy production and may serve as a regulator of mitochondrial protein synthesis, enhance the activity of the electron transport chain and protect the mitochondria against excessive ROS generation (14, 15, 17). Of importance to clinical outcomes, studies administering taurine via whole body supplementation or by applying directly to muscle preparations have found it effective at improving muscle health and/or force development (3, 7, 10, 35). Taurine deficiency has also been linked to cell damage associated with increased oxidative stress (15, 17). One interesting point is that in cardiomyocytes of rats depleted of taurine by beta-alanine, the activity of mitochondrial complex I and III, and thus the electron transport chain, was suppressed (17). This was supported by an apparent decrease in the abundance of complex I subunits ND5 and ND6, albeit in fractionated samples which presents problems as the total mitochondrial pool was not assessed (39).

To better understand the impact of disease severity and the potential of taurine as a substance of therapeutic benefit to DMD we investigated markers of mitochondrial content, activity and dynamics in the *mdx* mouse during both peak (28 d) and stable (70 d) pathology, using the same mice we described in a recent paper (3). Using whole muscle homogenates we investigated mitochondrial complexes in their native state by BN-PAGE, complex sub-units NDUFA9 and COX IV as protein indicators of mitochondrial content, citrate synthase (CS) as a measure of both mitochondrial content and activity, the abundance of fusion and fission proteins, Mfn2 and MiD49, respectively, as markers of mitochondrial dynamics and visualised mitochondrial distribution and abundance through confocal immunohistochemistry.

Materials & Methods

Animals and supplementation.

All procedures in this study were approved by the La Trobe University Animal Ethics Committee (approval numbers 12-31, 13-48). Only male mice were used with n=35 *mdx* and n=24 wild-type (WT, C57/BL10ScSn) animals in total. Experimental animals were bred at the La Trobe Animal Research and Teaching Facility using breeding pairs obtained from the Animal Resource Centre (Western Australia, Australia). The offspring of WT and *mdx* mice had access to standard rat chow, water *ad libitum* and were utilised for experimentation at either 28 ±1 or 70 ±1 days of age. Maximum litter size grown to maturity was 6 males. There was no significant difference between body weights of each age group at the age of experimentation (3). *Mdx* taurine (tau) breeders and subsequent offspring were supplemented with continuous access to taurine (2.5% wt/vol) enriched drinking water, with breeders beginning supplementation at least two weeks prior to mating. This dosage of supplementation has been demonstrated previously to elevate skeletal muscle taurine content in *mdx* mice (3).

Muscle dissection

Mice were anesthetised with an intraperitoneal injection of Nembutal (Sodium Pentobarbitone) and kept unresponsive to tactile stimuli while the *extensor digitorum longus* (EDL) and soleus muscles were excised, blotted clean on filter paper (Whatman No.1) and weighed, before being snap frozen in liquid nitrogen. All muscles were stored at -80°C until analysis. Mice were then killed by cardiac excision.

Western Blotting

Frozen transverse EDL and soleus cryosections were taken from the midpoint (~30 x 10 µm 28 d animals, ~20 x 10 µm 70 d animals) and immediately placed into a very low [Ca^{2+}] intracellular relaxing physiological buffer containing (in mM): 129 K^{+}, 36 Na^{+}, 1 free Mg^{2+} (10.3 total Mg^{2+}), 90 HEPES, 50 EGTA, 8 ATP, 10 CP, pH 7.10, and an osmolality of 295 ±10 mosmol·kg·H_2O^{-1}). The sections were then diluted 2:1 with 3X SDS solution (0.125 M Tris-HCl, 10% glycerol, 4% SDS, 4 M urea, 10% mercaptoethanol and 0.001% bromophenol blue, pH 6.8) and kept at room temperature for a further 30 minutes, vortexed at five minute intervals and stored at -80°C until analysed.

Aliquots of each EDL and soleus sample were pooled together and used to create a calibration curve for that respective muscle that was run on every gel, allowing comparisons of whole muscle homogenates across gels (25, 27). Total protein from each sample was initially separated on 4-15% gradient Criterion TGX Stain Free gels (BioRad, Hercules, CA) and following UV activation using a Stain Free Imager (BioRad), the densities of the total lanes were obtained (Image lab software v 5.2, BioRad) and used to ensure equal loading for subsequent western blotting.

Western blotting was performed to determine the protein abundance of mitochondrial proteins COX IV, NDUFA9, Mfn2 and MiD49. The western blotting protocol was similar to that described previously (26). Briefly, a similar amount of protein from skeletal muscle samples was separated on 4-15% gradient Criterion TGX Stain Free gels (BioRad, Hercules, CA). Prior to transfer gels were imaged with a Stain Free Imager (BioRad) for total protein which was quantified for each sample using Image lab software (v 5.2, BioRad). Following this, using a wet transfer protocol, protein was transferred onto a nitrocellulose membrane at 100V for 30 min. Following transfer the gel was imaged again and the membrane incubated in Pierce Miser solution (Pierce, Rockford, IL) for ~10 min and then blocked in 5% skim milk powder in 1% Tris-buffered, saline-Tween (TBST) for ~2 h at room temperature. Following blocking, membranes were incubated in primary antibodies overnight at 4°C and 2 h at room temperature. Antibody details and dilutions: cytochrome C oxidase subunit IV (COX IV, rabbit polyclonal, 1:1000, #4844, Cell Signalling), NADH:ubiquinone oxidotreductase subunit A9 (NDUFA9, rabbit polyclonal, 1:1000), Mfn2 (rabbit polyclonal,

1:500), MiD49 (rabbit polyclonal, 1:500, see (28, 31). *Mdx* mice were probed for dystrophin (mouse monoclonal, 1:500, MANDYS1 clone 3B7, Development Studies Hybridoma Bank (DSHB), Iowa, OH, USA) to confirm the absence of this protein. All antibodies were all diluted in 1% bovine serum albumin (BSA) in phosphate buffered saline (PBS) with 0.025% Tween (PBST).

After washing, membranes were incubated with a secondary antibody (goat anti-mouse IgG or IgM, goat anti-rabbit IgG, HRP conjugated, 1:60,000) and rinsed in TBST. Bands were visualized using West Femto chemiluminescent substrate (ThermoScientific, IL, USA) and images taken and densitometry performed using Image Lab software (BioRad). The positions of molecular mass markers were captured under white light, and then chemiluminescent imaging was taken without moving the membrane. Total protein and specific protein densities were each expressed relative to their respective calibration curves and subsequently each protein was normalised to the total protein content (27). Data was then expressed relative to the average of the 28 d WT on a given gel. Representative blots for figures have been created by superimposing blots on top of the molecular mass marker, with black lines indicating non congruent images from the same probe.

Citrate Synthase Activity Assay

For determination of citrate synthase (CS) activity, muscle was accurately weighed (10-21 mg) and homogenised (5 x 5 s, with 5 min on ice between bursts) at 20:1 in buffer containing 70 mM sucrose, 220 mM D-mannitol, 10 mM HEPES (pH 7.4), 1 mM EGTA. Measurements were made in whole muscle preparations in duplicate or triplicate. Placed into a reference cuvette was: 825 µL of 0.1 M Tris buffer, 100 µL of 5'5-dithiobis (2-nitrobenzoic acid) (DNTB, 0.5 $mg.mL^{-1}$ made in Tris buffer) and 10 µL of acetyl-coA (6 $mg.mL^{-1}$ made in Tris buffer). The cuvette was placed in a spectrophotometer (LKN Novaspec II, Pharmacia Biotech, Sweden) and the machine was zeroed at 412 nm. Into individual cuvettes containing the same components as the reference cuvette, 15 µL of homogenate was added in addition to 50 µL of oxaloacetate (6.1 $mg.mL^{-1}$ made in Tris buffer) to initiate the reaction. Absorbance was recorded at 412nm every 15s for a total of 150 s. The change in absorbance readings (Δ Abs) were plotted against time integrals (15 s) and linear

regression used to determine the slope of the response. The slope between 30 and 90 s was used to calculate CS activity, which is presented as $\mu mol \cdot min^{-1} \cdot g^{-1}$.

Blue Native PAGE (BN-PAGE)

To assess if mitochondrial complexes were present in their entirety we investigated mitochondrial complexes utilising BN-PAGE. Samples were cryo-sectioned and placed in Na-EGTA solution (described in whole muscle homogenate section) with 1% Triton-X100 (~30 x 10 µm 28 d animals, ~20 x 10 µm 70 d animals in 100 µL buffer). 10 µL of each sample were diluted 1:1 in solubilising solution (20 mM Bis-Tris pH 7.0, 50 mM NaCl, 10% glycerol, 0.5% Coomassie) with 2 µL of loading dye (5% Coomassie blue G, 500 mM ε-amino n-caproic acid, 100 mM Bis-Tris pH 7.0). Samples were loaded onto 4-13% native polyacrylamide gels (Novex, Invitrogen). Gels were run for 10 min at 100V, 10 min at 400V and a 45 min at 400V, with a change of buffer between the second and third run. Following separation, protein was transferred to PVDF membrane for 2 h at 100V. Membranes were stained (Coomassie blue G, 50% methanol, 10% acetic acid), destained (50% methanol, 10% acetic acid) and blocked for 2 h using 5% skim milk in TBST. Following blocking, the OXPHOS antibody cocktail (Mouse, 1:1000, Abcam) was applied and methodology from here to imaging is as described for Western blotting. Following imaging the remaining portions of the samples were diluted 1:2 in 3x SDS loading buffer and run on a 4-15% Stain-Free denaturing gel for the total protein used for quantification of each complex.

Immunohistochemistry (confocal microscopy)

To visualise COX IV and identify mitochondria in tissue sections, transverse cryosections (8-10 µm) were cut from the midpoint of the EDL and soleus muscles, and mounted on positively charged microscope slides (Lomb Scientific). Cryosections were left at room temperature for ~10 min, then the fixative (4% paraformaldehyde in PBS; PFA) added for 30 min. Afterwards, cryosections were washed (3 x 10 min in PBS), followed by immunobuffer (50 mM glycine, 0.033% saponin, 0.25% BSA, 0.05% sodium azide) and incubation for 2 hours. COX IV antibody (1:100, same source as western blotting), diluted in immunobuffer

was added and sections incubated overnight at room temperature in an airtight, saturated container. Sections were washed with immunobuffer (3 x 10 min), before secondary antibody (1:2000 in immunobuffer, Donkey anti-rabbit Alexis 488 (Abcam, ab150061)) was added and sections incubated for 2 hours at room temperature. Sections were then washed in immunobuffer (10 min) before adding DAPI (1:1000 in immunobuffer, 2 min) for visualizing nuclei. A negative control slide was obtained by following the above steps with the omission of primary antibody, where immunobuffer was used during that incubation step. Sections were finally washed (2 x 10 min, PBS) before being air-dried, and a coverslip carefully applied with a drop of ProLong Diamond Antifade Mountant (Thermo Fisher, P36961), and the coverslip sealed with nail polish. Fluorescently labelled samples were stored in the dark at -20℃. Images were all taken at the same magnification with a Zeiss 780 confocal laser-scanning microscope (Zeiss AxioObserver Z1, Carl Zeiss Microscopy, Oberkochen, Germany).

Statistics

All data are presented as mean ± standard deviation (SD). Comparisons between relevant groups was performed using a One-way ANOVA of variance, with Holm-Sidak's post-hoc analyses. All statistical analysis was performed using GraphPad Prism v 6. Significance was set at $p < 0.05$.

Results

Mitochondrial complex I, II, IV and V abundances

The abundance of mitochondrial complexes were assessed using BN-PAGE with duplicate measurements of each sample. No difference in the abundances or the apparent migrations of complexes I, II, IV or V were found in the soleus muscle of WT, *mdx and mdx* Tau mice (Fig 1).

NDUFA9 and COX IV protein.

In soleus muscle the mitochondrial marker associated with complex I, NDUFA9, was decreased by approximately 50% in *mdx* mice at both 28 and 70 d compared to age matched WT mice (Fig 1A). 70 d *mdx* tau mice exhibited an approximate 50% increase in NDUFA9 protein abundance when compared to the *mdx* group, this increase was not observed between 28 d *mdx* and *mdx* tau supplemented mice (Fig 2A). NDUFA9 abundance was elevated significantly with age in both the WT and *mdx* groups (Fig 2A). EDL NDUFA9 protein abundance was reduced in 28 d *mdx* mice when compared to the WT, with no further differences observed with NDUFA9 protein abundance between groups (Fig 2B). There was no differences in soleus or EDL COX IV protein abundances between any groups (Fig 2C-D).

Citrate synthase activity.

The enzyme citrate synthase is a validated biomarker for mitochondrial density in skeletal muscle, and CS activity is widely used as measure of oxidative capacity (19) and thereby was used in the current study. There was an age specific effect on soleus CS activity, with 70 d old WT, *mdx* and *mdx* tau mice all exhibiting more than two-fold increase relative to the 28 d animals from the same group (Fig 3A). There were no group specific differences in EDL CS activity at either 28 or70 d (Fig 3B). There was approximately 20% less CS activity in 28 d *mdx* compared with WT mice, with no further differences observed between groups or ages (Fig 3B).

Mitochondrial dynamics, Mfn2 and MiD49, proteins.

There were no differences observed in the abundance of Mfn2 and MiD49 proteins in either soleus or EDL muscles in any group (Fig 4).

Immunohistochemistry

Mitochondrial abundance following immunostaining was visualised using confocal microscopy. Staining of muscle sections with COX IV antibody revealed a qualitatively similar abundance of mitochondria across all treatment types (Fig. 5), as observed by western blot analysis (Fig. 2). There was no discernible difference in staining intensity between the EDL and soleus muscles of 28 d mice, but there was heterogeneity of COX IV staining intensity observed between muscle fibres. Presumably greater COX IV, and therefore mitochondria, is present in the slow twitch oxidative fibres while a lesser intensity is presented in the more glycolytic fast twitch fibers.

DAPI stain revealed a higher abundance of centralised myonuclei and infiltration of other nuclei in both EDL and soleus muscles of 28 d *mdx* mice, which were present to a lesser extent in *mdx* tau treated and WT mice (Fig. 5). This trend was not observed in the soleus muscle of 70 d mice (Fig. 5).

Discussion

The current study provides muscle specific insights into the effect of age on mitochondria in wild-type and the *mdx* mouse model of DMD. It also addresses whether the benefits of taurine supplementation on muscle function (3) are due to changes in mitochondrial content or activity.

We investigated the abundance of whole mitochondrial respiratory complexes I, II, IV and V in their native state by BN-PAGE and found no differences in the abundances or the relative migration of these complexes between WT and *mdx* mice in either 28 d animals, when the dystrophic phenotype would be active and the most damage occurring, or during stable stages of muscle damage at 70 d (Fig 1B). The examination of mitochondrial complexes by BN-PAGE has the advantage of providing information about not only complex abundance but the formation of individual complexes. Each complex consists of numerous individual proteins, e.g. complex I has 45 subunits and migrates at ~1,000 kDa when containing its full complement of protein subunits (38). These data suggest that at least the majority of the subunits assembled for a given complex, are similar between phenotype and ages.

Given that no differences were seen in mitochondrial complexes, we then went on to examine two important markers of mitochondrial complex abundance by western blotting using calibration curves and small sample amounts, which provide the most quantitative approach (27). The protein NDUFA9 is one of the 45 subunits that comprise mammalian complex I (24) and has been used previously as a marker of both complex abundance and total mitochondrial content (39). Interestingly, there was ~two-fold less NDUFA9 protein in soleus muscle from *mdx* mice at both 28 and 70 d compared with WT mice (Fig 2A). In EDL muscle this was only seen in 70 d animals (Fig 2B). In soleus muscles from both WT and *mdx* mice there was ~two-fold increase in NDUFA9 abundances with age (Fig 2A). Given that NDUFA9 is an ~36 kDa protein, then on its own, it would not be expected to be observed as a difference in the migration or the abundance of the total Complex I on BN-PAGE. Whilst NDUFA9 is part of Complex I, it is unclear if a change in its abundance would affect overall mitochondrial function (24). However the decrease in NDUFA9 protein abundance found here does coincide with reports of a deficiency in Complex I function that was apparent in muscle from *mdx* compared with WT animals (32). It was pleasing that the mitochondrial

yields were reported in that paper and worth due consideration was the low mitochondrial yields (10-18%) and a difference in the yields between muscle from *mdx* and WT mice (32). Interestingly, in cardiac muscle from *mdx* mice cardiomyocytes have been shown to exhibit altered mitochondrial activity that was not evident at the level of isolated mitochondria, suggesting the problem exists on a cellular as opposed to organelle level (36). Such studies highlight the importance of investigating mitochondrial function in the context of its role within the cell as well as in isolation. An important and novel aspect of our study is the use of whole muscle for all our biochemical analyses including BN-PAGE, western blotting and CS activity. Studies undertaking mitochondrial research involving centrifugation of tissue samples may be underestimating mitochondrial content, as recently Wyckelsma et al. (39) identified approximately 10-40% of mitochondria are discarded and, very importantly, the yields were different when measuring different mitochondrial proteins and different samples were used. A further and more detailed description of the issues associated with quantitative assessment following fractionation of tissue are reported by Murphy and Lamb (27).

Our second protein marker of mitochondrial abundance was COX IV, has been established as being essential for complex IV (Cytochrome-c oxidase) function (20). We found no difference in the protein abundance of COX IV between *mdx* and WT groups in both soleus and EDL muscle at both ages (Fig 2D). This, in combination with BN-PAGE data, suggests that Complex IV is not altered in dystrophic muscle, or as a consequence of age. Qualitative visualisation of COX IV through confocal microscopy further confirmed these results, revealing no appreciable difference between muscle types, age and tau treatment (Fig 5). There was however a fibre specific heterogeneity in the intensity of COX IV, with greater intensity observed in presumably type I slow twitch oxidative fibres as opposed to glycolytic type II fibres (Fig 5).

Shown to be strongly associated with mitochondrial content and the ability of the mitochondria to produce ATP (oxidative capacity) (19), we also investigated CS activity in muscles from the *mdx* and WT animals at both ages. We found no change in CS activity when comparing soleus muscle from *mdx* and WT mice, either at 28 or 70 d (Fig 3A). When the effect of age was examined in soleus muscles, CS activity was increased ~two-fold in

both *mdx* and WT mice 70 d mice compared to their respective 28 d mice (Fig 3). Interestingly this age specific increase was of similar magnitude to that observed in NDUFA9 protein abundance (Fig 2A). Whilst it is tempting to speculate that the NDUFA9 protein abundance is either responding to or driving the age dependent increase in oxidative capacity of Complex I in soleus muscle, it cannot explain the decreased NDUFA9 protein abundance seen in soleus muscle of *mdx* compared with WT mice. It is clear that further studies are required to elucidate the reason behind the age related changes in CS activity.

This is the first work to investigate the abundance of the mitochondrial specific dynamics proteins, Mfn2 and MiD49, in whole skeletal muscle from the *mdx* mouse. There were no differences in protein abundances of either Mfn2 or MiD49 across both soleus and EDL muscles and across groups (Fig 4). Based on the previously published suggestion that total oxidative capacity (measured as MAPR and OXPHOS) may be reduced in *mdx* mice, we had thought mitochondrial dynamics would be increased. It was surprising, therefore, to see that there was no evidence of altered abundance in Mfn2 or MiD49 in the *mdx* mouse during 28 d where the period where peak muscular damage occurs and muscle turnover is high. Interestingly, a recent study reported a several-fold increase in the abundance of Mfn2 in the EDL muscle of 8 week old utrophin-dystrophin deficient mouse (29). The utrophin-dystrophin deficient mouse model cannot be directly compared with the less severe *mdx* mouse model because it experiences a more severe phenotype of muscle damage. Those data provide evidence, however, that Mfn2can be upregulated in a compensatory capacity in response to either increased mitochondrial damage or energy demand that was not seen in the present study. That study also found an increase in Drp1 (29), although given that Drp1 is involved with the fission of peroxisomes as well as mitochondria, it limits the interpretation of that finding in relation specifically to mitochondria. We have recently reported both Mfn2 and MiD49 to be increased in muscle from aged compared with young adults, further supporting the dynamic response of these proteins (39).

Previously we identified that taurine supplementation was effective at increasing strength and improving the histological profile of the *tibialis anterior* muscle in *mdx* mice during the peak damage period of 28 d utilising the same mice and treatment regime as the present study (3). In the current study we investigated whether the beneficial effects of taurine

were associated with an increase in markers of oxidative capacity or mitochondrial abundance. Visualisation of nuclei using fluorescent DAPI staining revealed taurine to have a seemingly beneficial effect on the visible health of EDL and soleus muscles of 28 d *mdx* taurine treated mice, as seen with hematoxylin and eosin staining (3). However, while an increase in NDUFA9 protein abundance was observed in the 70 d *mdx* tau mouse when compared to the non-supplemented *mdx* mouse there was no effect of taurine on any other measure of mitochondrial content or activity. While our current data suggests that taurine affords no mitochondrial adaptation in the *mdx* mouse at either 28 or 70 d of age, it remains that complex I activity can be selectively impaired without detectable changes in complex content or mitochondrial volume/density. Subsequently a possible mechanism for functional improvement with taurine supplementation could be a reduction in the impairment of electron transport secondary to an antioxidant effect at complex I (17). It is thereby not wholly conclusive in the current study that taurine supplementation did not elicit some mitochondrial adaptation which requires further investigation. Future studies should assess mitochondrial function *in situ* and include high-resolution respirometry, while ultrastructural mitochondrial reticular comparison would be of interest to support or refute the relevance of absolute measures of Mfn2 and MiD49 for mitochondrial dynamics.

Conclusion

Our assessment of mitochondria using an array of approaches (BN-PAGE, western blotting, confocal microscopy and CS activity) suggest there is no reason to believe that mitochondrial content is reduced in *mdx* mouse, at either 28 d when peak damage is occurring, or at 70 d when the muscle is stabilised. In order to further elucidate this, there is an absolute need for future functional mitochondria assays to be undertaken in whole muscle preparations, where the entire mitochondrial pool are represented.

Acknowledgements

We would like to acknowledge Dr. Peter Lock and the LIMS BioImaging facility for assistance with obtaining the confocal images used in the present study.

Figure Legends

Figure 1. Native state complex abundance in soleus muscle of 28 and 70 d WT, *mdx* and *mdx* tau mice. (A) Myosin from the Stain Free gel, indicative of total protein (*top*), Representative blot of Blue Native PAGE using OXPHOS cocktail antibody (*bottom*). **(B)** Complex I, II, IV and V abundances normalised to the average of the 28 d WT from 28 d (solid symbols) and 70 d (open symbols) WT (circles), *mdx* (triangles) and *mdx* tau (squares) mice. One way ANOVA with Holm-Sidak's post-hoc analyses between relevant groups. Data presented as data points surrounding means ± SD, n indicated by number of symbols.

Figure 2. Mitochondrial protein abundance in soleus and EDL muscles of 28 and 70 d WT, *mdx* and *mdx* tau mice. Shown for each panel is the myosin from the Stain Free gel, indicative of total protein (*top),* the representative Western blot protein (*middle*), and quantification of protein abundance (*bottom*) from 28 d (solid symbols) and 70 d (open symbols) WT (circles), *mdx* (triangles) and *mdx* tau (squares) mice. NDUFA9 in soleus **(A)** and EDL **(B)** and COX IV in soleus **(C)** and EDL **(D)**, each expressed relative to the 28 d WT. One way ANOVA with Holm-Sidak's post-hoc analyses between relevant groups. Data presented as data points surrounding means ± SD, n indicated by number of symbols. Lines connecting different bars indicate significance at $p<0.05$, *** $p<0.001$.

Figure 3. Citrate synthase activity in soleus and EDL muscles of 28 d compared 70 d wild-type, *mdx* and *mdx* taurine (*mdx* tau) mice. (A) Soleus citrate synthase activity **(B)** EDL citrate synthase activity assay from 28 d (solid symbols) and 70 d (open symbols) WT (circles), *mdx* (triangles) and *mdx* tau (squares) mice. One way ANOVA with Holm-Sidak's post-hoc analyses between relevant groups. Data presented as data points surrounding means ± SD, n indicated by number of symbols. Lines connecting different bars indicate significance at * $p<0.05$, *** $p<0.001$.

Figure 4. Mitochondrial dynamics protein abundance in soleus and EDL muscles of 28 and 70 d WT, *mdx* and *mdx* tau mice. Shown for each panel is the myosin from the Stain Free gel, indicative of total protein (*top),* the representative Western blot protein (*middle*), and quantification of protein abundance (*bottom*) from 28 d (solid symbols) and 70 d (open symbols) WT (circles), *mdx* (triangles) and *mdx* tau (squares) mice. **(A)** Fa9, **(B)** COX IV, **(C)** MfN2 and **(D)** MiD49 expressed relative to the 28 d WT. One way ANOVA with Holm-Sidak's post-hoc analyses between relevant groups. Data presented as data points surrounding means ± SD, n indicated by number of symbols. Lines connecting different bars indicate significance at $p<0.05$.

Figure 5. Confocal microscopy imaging of mitochondria and nuclei in 28 d and 70 d wild-type, *mdx* and *mdx* taurine mice. Transverse sections of EDL and soleus muscles from 28 and 70 d WT, *mdx* and *mdx* tau mice shown at 400 X magnification by confocal laser scanning microscope. Nuclei are stained blue (DAPI), mitochondria are stained green (COX IV protein). Greater intensity of color equates to greater abundance of COX IV. Fiber outlines are evident. Scale bars = 100 µm. Experiments repeated on n = 4 animals for all groups.

References

1. **Allen DG, Whitehead NP, and Froehner SC**. Absence of Dystrophin Disrupts Skeletal Muscle Signaling: Roles of Ca2+, Reactive Oxygen Species, and Nitric Oxide in the Development of Muscular Dystrophy. *Physiol Rev* 96: 253-305, 2016.
2. **Austin L, de Niese M, McGregor A, Arthur H, Gurusinghe A, and Gould MK**. Potential oxyradical damage and energy status in individual muscle fibres from degenerating muscle diseases. *Neuromuscular Disorders* 2: 27-33, 1992.
3. **Barker RG, Horvath D, van der Poel C, and Murphy RM**. Benefits of Pre-natal Taurine Supplementation in Preventing the Onset of Acute Damage in the Mdx Mouse. *PLOS Currents Muscular Dystrophy* 2017 doi: 10.1371/currents.md.9a3e357a0154d01050b591601cbd4fdb.
4. **Brookes PS, Yoon Y, Robotham JL, Anders MW, and Sheu SS**. Calcium, ATP, and ROS: a mitochondrial love-hate triangle. *Am J Physiol Cell Physiol* 287: C817-833, 2004.
5. **Bushby K, Finkel R, Birnkrant DJ, Case LE, Clemens PR, Cripe L, Kaul A, Kinnett K, McDonald C, Pandya S, Poysky J, Shapiro F, Tomezsko J, and Constantin C**. Diagnosis and management of Duchenne muscular dystrophy, part 1: diagnosis, and pharmacological and psychosocial management. *Lancet Neurology* 9: 77-93, 2010.
6. **Cole MA, Rafael JA, Taylor DJ, Lodi R, Davies KE, and Styles P**. A quantitative study of bioenergetics in skeletal muscle lacking utrophin and dystrophin. *Neuromuscular disorders* 12: 247-257, 2002.
7. **Cozzoli A, Rolland JF, Capogrosso RF, Sblendorio VT, Longo V, Simonetti S, Nico B, and De Luca A**. Evaluation of potential synergistic action of a combined treatment with alpha-methyl-prednisolone and taurine on the mdx mouse model of Duchenne muscular dystrophy. *Neuropathology and Applied Neurobiology* 37: 243-256, 2011.
8. **Crompton M**. The mitochondrial permeability transition pore and its role in cell death. *Biochem J* 341: 233-249, 1999.
9. **De Luca A, Pierno S, and Camerino DC**. Taurine: the appeal of a safe amino acid for skeletal muscle disorders. *Journal of translational medicine* 13: 243, 2015.
10. **De Luca A, Pierno S, Liantonio A, Cetrone M, Camerino C, Fraysse B, Mirabella M, Servidei S, Ruegg UT, and Conte Camerino D**. Enhanced dystrophic progression in mdx mice by exercise and beneficial effects of taurine and insulin-like growth factor-1. *J Pharmacol Exp Ther* 304: 453-463, 2003.
11. **Griffin JL, Williams HJ, Sang E, Clarke K, Rae C, and Nicholson JK**. Metabolic Profiling of Genetic Disorders: A Multitissue 1H Nuclear Magnetic Resonance Spectroscopic and Pattern Recognition Study into Dystrophic Tissue. *Analytical biochemistry* 293: 16-21, 2001.
12. **Grounds MD, Radley HG, Lynch GS, Nagaraju K, and De Luca A**. Towards developing standard operating procedures for pre-clinical testing in the mdx mouse model of Duchenne muscular dystrophy. *Neurobiol Disease* 31: 1-19, 2008.
13. **Gunter TE, Yule DI, Gunter KK, Eliseev RA, and Salter JD**. Calcium and mitochondria. *FEBS Lett* 567: 96-102, 2004.
14. **Hansen SH, Andersen ML, Birkedal H, Cornett C, and Wibrand F**. The important role of taurine in oxidative metabolism. *Adv Exp Med Biol* 583: 129-135, 2006.
15. **Hansen SH, Andersen ML, Cornett C, Gradinaru R, and Grunnet N**. A role for taurine in mitochondrial function. *J Biomedical Science* 17 Suppl 1: S23, 2010.
16. **Huxtable RJ**. Physiological actions of taurine. *Physiological reviews* 72: 101-163, 1992.
17. **Jong CJ, Azuma J, and Schaffer S**. Mechanism underlying the antioxidant activity of taurine: prevention of mitochondrial oxidant production. *Amino Acids* 42: 2223-2232, 2012.
18. **Kuznetsov AV, Winkler K, Wiedemann F, von Bossanyi P, Dietzmann K, and Kunz WS**. Impaired mitochondrial oxidative phosphorylation in skeletal muscle of the dystrophin-deficient mdx mouse. *Mol Cell Biochem* 183: 87-96, 1998.

19. **Larsen S, Nielsen J, Hansen CN, Nielsen LB, Wibrand F, Stride N, Schroder HD, Boushel R, Helge JW, Dela F, and Hey-Mogensen M**. Biomarkers of mitochondrial content in skeletal muscle of healthy young human subjects. *J Physiol* 590: 3349-3360, 2012.
20. **Li Y, Park J-S, Deng J-H, and Bai Y**. Cytochrome c oxidase subunit IV is essential for assembly and respiratory function of the enzyme complex. *J Bioenergetics Biomembranes* 38: 283-291, 2006.
21. **Loson OC, Song Z, Chen H, and Chan DC**. Fis1, Mff, MiD49, and MiD51 mediate Drp1 recruitment in mitochondrial fission. *Mol Biol Cell* 24: 659-667, 2013.
22. **McIntosh L, Granberg KE, Briere KM, and Anderson JE**. Nuclear magnetic resonance spectroscopy study of muscle growth, mdx dystrophy and glucocorticoid treatments: correlation with repair. *NMR Biomedicine* 11: 1-10, 1998.
23. **Millay DP, Sargent MA, Osinska H, Baines CP, Barton ER, Vuagniaux G, Sweeney HL, Robbins J, and Molkentin JD**. Genetic and pharmacologic inhibition of mitochondrial-dependent necrosis attenuates muscular dystrophy. *Nature Med* 14: 442-447, 2008.
24. **Mimaki M, Wang X, McKenzie M, Thorburn DR, and Ryan MT**. Understanding mitochondrial complex I assembly in health and disease. *Biochimica et Biophysica Acta (BBA) - Bioenergetics* 1817: 851-862, 2012.
25. **Mollica JP, Oakhill JS, Lamb GD, and Murphy RM**. Are genuine changes in protein expression being overlooked? Reassessing Western blotting. *Anal Biochem* 386: 270-275, 2009.
26. **Murphy RM**. Enhanced technique to measure proteins in single segments of human skeletal muscle fibers: fiber-type dependence of AMPK-alpha1 and -beta1. *J Appl Physiol (1985)* 110: 820-825, 2011.
27. **Murphy RM, and Lamb GD**. Important considerations for protein analyses using antibody based techniques: down-sizing Western blotting up-sizes outcomes. *J Physiol* 591: 5823-5831, 2013.
28. **Osellame LD, Singh AP, Stroud DA, Palmer CS, Stojanovski D, Ramachandran R, and Ryan MT**. Cooperative and independent roles of the Drp1 adaptors Mff, MiD49 and MiD51 in mitochondrial fission. *J Cell Sci* 129: 2170-2181, 2016.
29. **Pant M, Sopariwala DH, Bal NC, Lowe J, Delfin DA, Rafael-Fortney J, and Periasamy M**. Metabolic dysfunction and altered mitochondrial dynamics in the utrophin-dystrophin deficient mouse model of duchenne muscular dystrophy. *PloS One* 10: e0123875, 2015.
30. **Percival JM, Siegel MP, Knowels G, and Marcinek DJ**. Defects in mitochondrial localization and ATP synthesis in the mdx mouse model of Duchenne muscular dystrophy are not alleviated by PDE5 inhibition. *Human Mol Genetics* 22: 153-167, 2013.
31. **Richter V, Palmer CS, Osellame LD, Singh AP, Elgass K, Stroud DA, Sesaki H, Kvansakul M, and Ryan MT**. Structural and functional analysis of MiD51, a dynamin receptor required for mitochondrial fission. *J Cell Biol* 204: 477-486, 2014.
32. **Rybalka E, Timpani CA, Cooke MB, Williams AD, and Hayes A**. Defects in mitochondrial ATP synthesis in dystrophin-deficient mdx skeletal muscles may be caused by complex I insufficiency. *PloS One* 9: e115763, 2014.
33. **Sebastian D, Sorianello E, Segales J, Irazoki A, Ruiz-Bonilla V, Sala D, Planet E, Berenguer-Llergo A, Munoz JP, Sanchez-Feutrie M, Plana N, Hernandez-Alvarez MI, Serrano AL, Palacin M, and Zorzano A**. Mfn2 deficiency links age-related sarcopenia and impaired autophagy to activation of an adaptive mitophagy pathway. *EMBO J* 35: 1677-1693, 2016.
34. **Terrill JR, Grounds MD, and Arthur PG**. Taurine deficiency, synthesis and transport in the mdx mouse model for Duchenne Muscular Dystrophy. *Int J Biochem; Cell Biology* 66: 141-148, 2015.
35. **Terrill JR, Pinniger GJ, Graves JA, Grounds MD, and Arthur PG**. Increasing taurine intake and taurine synthesis improves skeletal muscle function in the mdx mouse model for Duchenne muscular dystrophy. *J Physiol* 594: 3095-3110, 2016.
36. **Viola HM, Davies SM, Filipovska A, and Hool LC**. L-type Ca(2+) channel contributes to alterations in mitochondrial calcium handling in the mdx ventricular myocyte. *Am J Physiol Heart Circ Physiol* 304: H767-775, 2013.

37. **Warskulat U, Flögel U, Jacoby C, Hartwig H, Thewissen M, Merx MW, Molojavyi A, Heller-Stilb B, Schrader J, and Häussinger D**. Taurine transporter knockout depletes muscle taurine levels and results in severe skeletal muscle impairment but leaves cardiac function uncompromised. *FASEB J* 18: 577-579, 2004.
38. **Wittig I, Braun H-P, and Schagger H**. Blue native PAGE. *Nature Protocols* 1: 418, 2006.
39. **Wyckelsma VL, Levinger I, McKenna MJ, Formosa LE, Ryan MT, Petersen AC, Anderson MJ, and Murphy RM**. Preservation of skeletal muscle mitochondrial content in older adults:relationship between mitochondria, fibre-type & high intensity exercise training. *J Physiol* 595(11):3345-3359 2017.

A

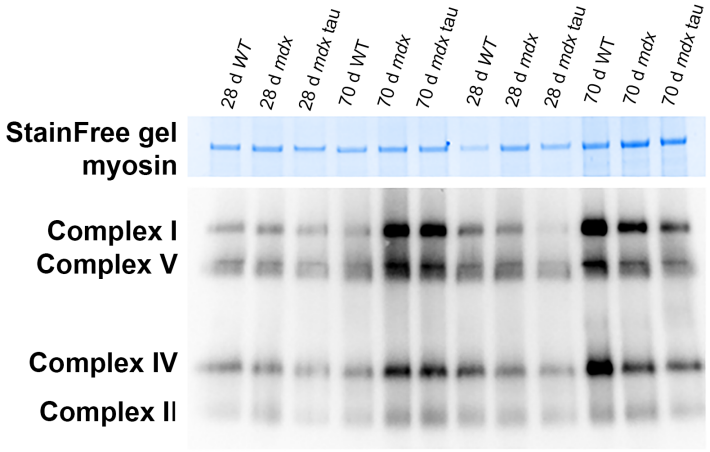
28 d WT
28 d mdx
28 d mdx tau
70 d WT
70 d mdx
70 d mdx tau
28 d WT
28 d mdx
28 d mdx tau
70 d WT
70 d mdx
70 d mdx tau
StainFree gel myosin
Complex I
Complex V
Complex IV
Complex II

B

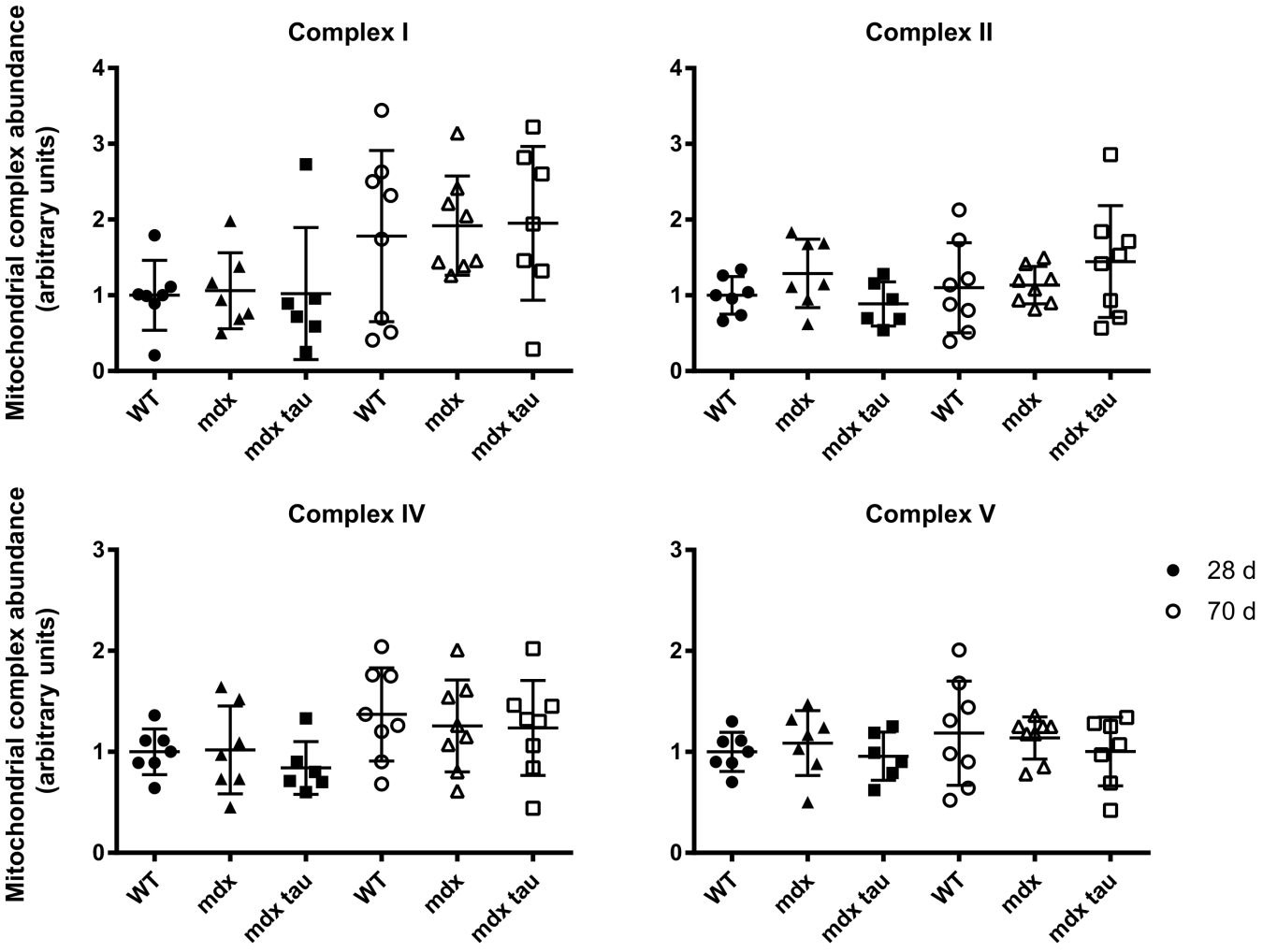
Complex I
Complex II
Complex IV
Complex V
Mitochondrial complex abundance (arbitrary units)
Mitochondrial complex abundance (arbitrary units)
0
1
2
3
4
WT
mdx
mdx tau
WT
mdx
mdx tau
28 d
70 d

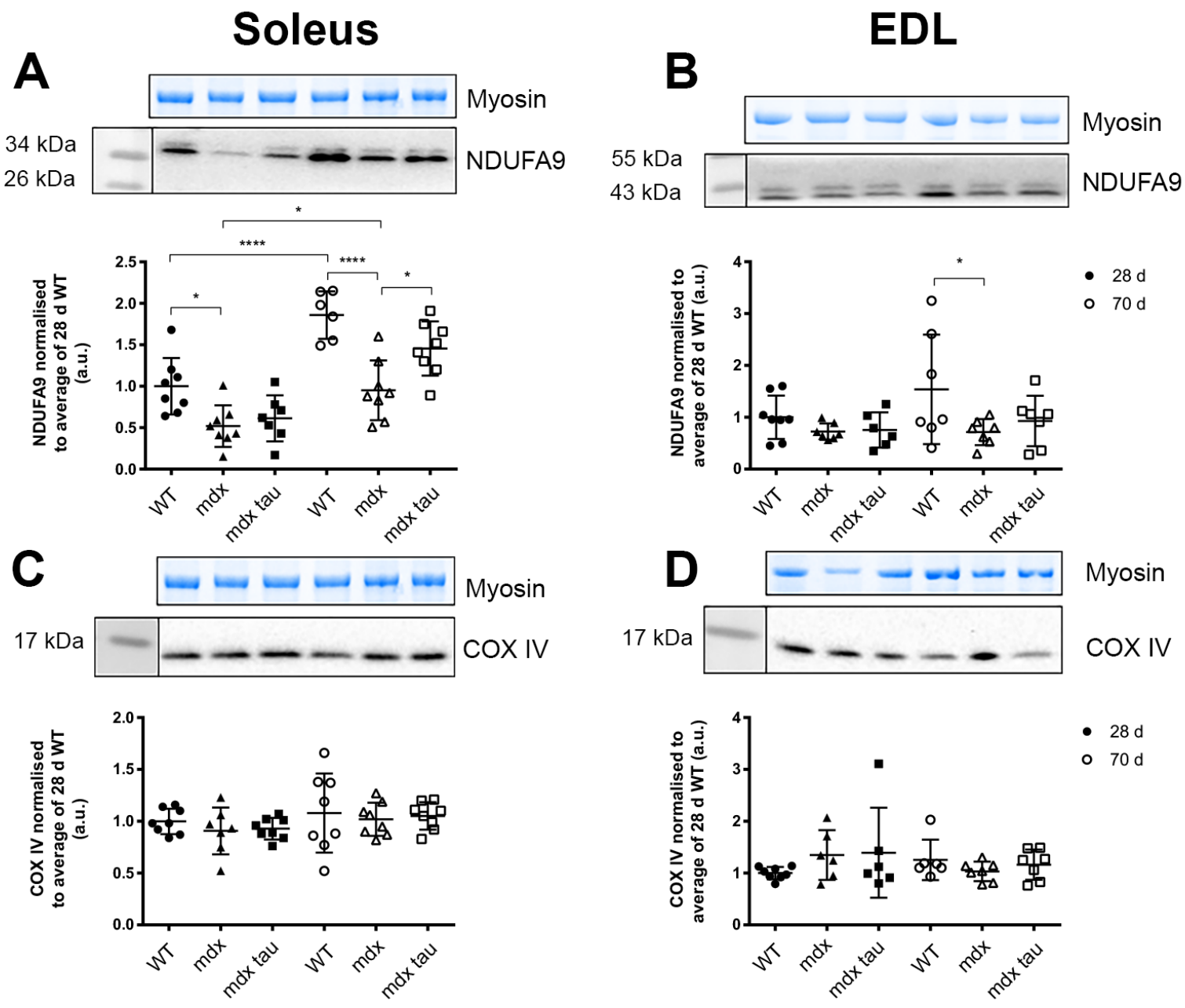
Soleus
EDL
A
B
C
D
Myosin
NDUFA9
34 kDa
26 kDa
55 kDa
43 kDa
17 kDa
COX IV
NDUFA9 normalised to average of 28 d WT (a.u.)
COX IV normalised to average of 28 d WT (a.u.)
28 d
70 d
WT
mdx
mdx tau

A

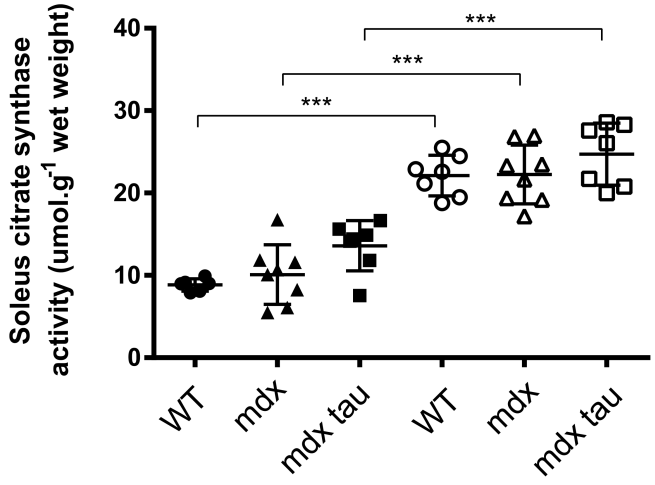
Soleus citrate synthase activity (umol.g-1 wet weight)
40
30
20
10
0
***
***
***
WT
mdx
mdx tau
WT
mdx
mdx tau

B

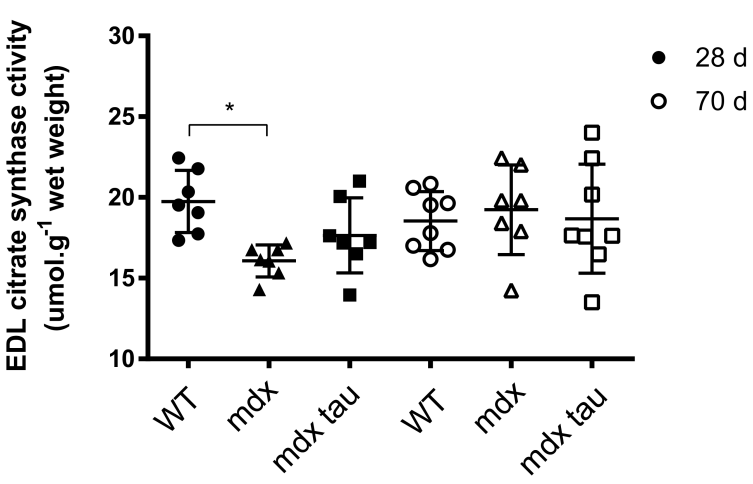
EDL citrate synthase ctivity (umol.g-1 wet weight)
30
25
20
15
10
*
28 d
70 d
WT
mdx
mdx tau
WT
mdx
mdx tau

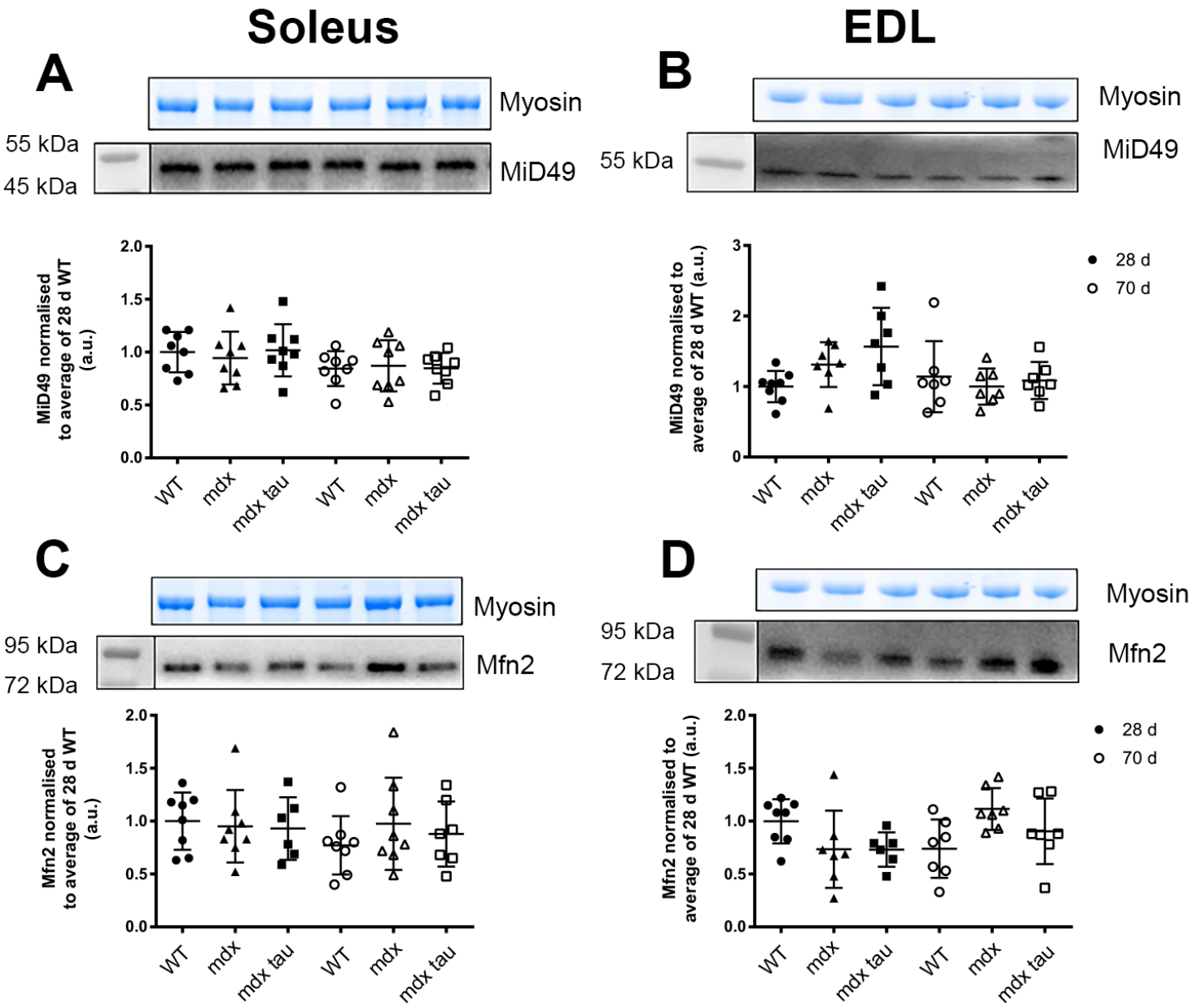
Soleus
EDL
A
B
C
D
Myosin
MiD49
Mfn2
55 kDa
45 kDa
95 kDa
72 kDa
MiD49 normalised to average of 28 d WT (a.u.)
Mfn2 normalised to average of 28 d WT (a.u.)
28 d
70 d
WT
mdx
mdx tau

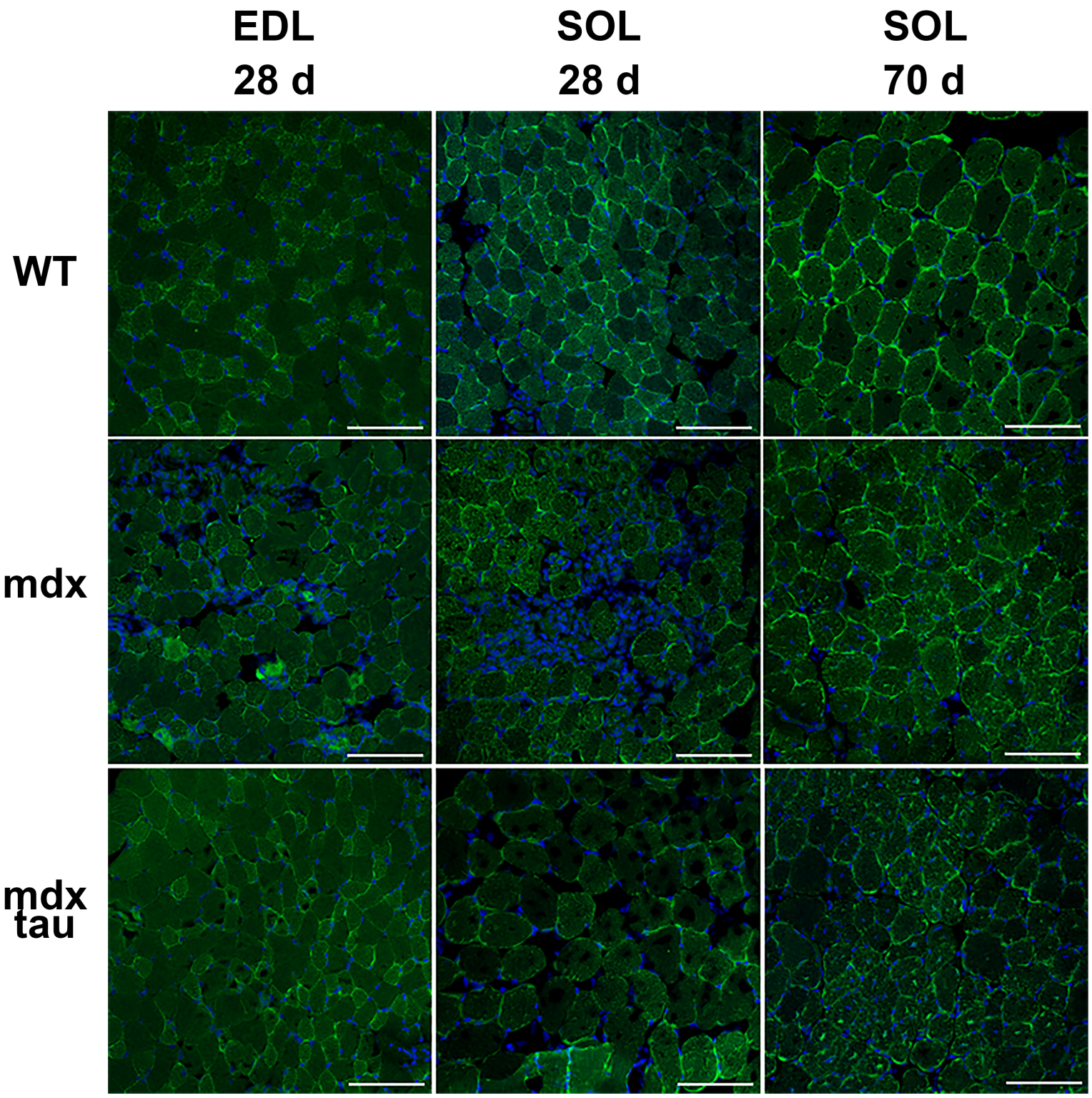
EDL
28 d
SOL
28 d
SOL
70 d
WT
mdx
mdx
tau